Journal of Advanced Concrete Technology
Materials, Structures and Environment

Study of using dolomite as starting material resource to produce magnesium oxychloride cement

Mahmut Altiner, Mehmet Yildirim

Journal of Advanced Concrete Technology, volume 15 (2017), pp. 269-277

Related Papers Click to Download full PDF!

Sodium and Magnesium Sulfate Resistance of Mortars with Interground Limestone and Limestone Powder Replacing Cements

Ittiporn Sirisawat, Lalita Baingam, Warangkana Saengsoy, Pitisan Krammart, Somnuk Tangtermsirikul

Journal of Advanced Concrete Technology, volume 12 (2014), pp. 403-412

Click to Submit your Papers

Japan Concrete Institute http://www.j-act.org

Scientific paper

Study of using Dolomite as Starting Material Resource to Produce Magnesium Oxychloride Cement

Mahmut Altiner[1*] and Mehmet Yildirim[2]

Received 25 March 2017, accepted 1 June 2017 doi:10.3151/jact.15.269

Abstract

In this paper, the starting materials necessary for producing magnesium oxychloride cement (MOC) were produced from dolomite ore using leaching-carbonation-evaporation-pyrohydrolysis processes. The influences of the molar ratio of $MgO/MgCl_2$ (M_x) and $H_2O/MgCl_2$ (H_y) on the properties of the MOC (cured for 7 days) were determined using physico-mechanical methods. SEM and XRD analyses were conducted to determine the change of phase and microstructure of the selected 7-day MOC depending on the production conduction. The experimental results show that the best mix proportion of 7-day MOC was found to be $M_{6.06}H_{14}$ and its thermal conductivity, flexural strength, and compressive strength values were found to be 1.202 W/mK, 4.22 MPa, and 87.7 MPa, respectively. The water resistance of the MOC was improved by a small amount of H_3PO_4 (4% of MgO by weight). Consequently, if MOC is produced from dolomite, high-purity synthetic aragonite and CO_2 would be obtained as byproducts, which are strongly demanded.

1. Introduction

Cement is one of the most important building materials and has accelerated industrialization and modernization. However, during cement production, CO_2 gas is released into the atmosphere because of the calcination of limestone ($CaCO_3$). The production of 1 t of cement generates 0.9 t of CO_2 as a byproduct (Hendriks *et al*. 2004), which represents approximately 6–8% of all anthropogenic carbon emissions. The amount of cement produced between 2005 and 2016 is 71.5×10^6 t, and approximately 64×10^6 t of CO_2 was released in this period on the basis of this ratio. The amount of CO_2 emitted as a result of cement production has been projected to increase two or three times by 2050 relative to the amount emitted in 2010 unless the cement production method is improved (Imbabi *et al*. 2012).

The Kyoto Protocol was established in 1997 to reduce the emissions of gases that trigger global warming. As of 2009, 181 countries signed it and, as a party to the protocol, are responsible for reducing or limiting emissions by 2020. CO_2 is one of the gases responsible for the greenhouse effect. Low-carbon-based cement is an opportunity to reduce the amount of CO_2 generated during cement production.

Many studies have been carried out to prepare carbon-negative cement composites for reducing CO_2 emissions released into the atmosphere as a result of the cement manufacturing process. One such composite is magnesium oxychloride (MOC, known as Sorel cement), which is produced through neutralizing–hydrolyzing–crystallizing reactions in the ternary system of magnesium chloride solution ($MgCl_2$)–magnesium oxide (MgO) powder–water (H_2O) (Dehua and Chuanmei 1999). The properties of MOC are strongly influenced by the $MgO/MgCl_2$ and $H_2O/MgCl_2$ molar ratios (Chau and Li 2007; Li and Chau 2007; Xu *et al*. 2016), magnesia reactivity (Harper 1967; Chau and Li 2008; Zhu *et al*. 2013) and curing temperature (Sglavo *et al*. 2011). Depending on these parameters, four types of MOC can be obtained: phase 2 ($2Mg(OH)_2{\cdot}MgCl_2{\cdot}4H_2O$, P2), phase 3 ($3Mg(OH)_2{\cdot}MgCl_2{\cdot}8H_2O$, P3), phase 5 ($5Mg(OH)_2{\cdot}MgCl_2{\cdot}8H_2O$, P5), and phase 9 ($9Mg(OH)_2{\cdot}MgCl_2{\cdot}H_2O$, P9) (Sorel 1867).

Among the aforementioned four types of reaction products, P5 is believed to be the most desirable product because it exhibits better mechanical properties than P2, P3, and P9. Unfortunately, the use of MOC in engineering applications is limited because of its poor water resistance. When an MOC was immersed in water for a certain period, needle-like P5 decomposed to Mg(OH)2, which leads to a greater than 80% decrease in the compressive strength of the MOC (Qiao *et al*. 2014) because of the formation of a highly porous structure (Zhang and Deng 1994). Luckily, previous studies have already identified a method to improve the water resistance of MOC by adding a small amount of a modifier such as citric acid ($C_6H_8O_7$) (Wen *et al*. 2014), phosphate (Deng 2003; Tan *et al*. 2014; Wu. *et al*. 2015; Qiao *et al*. 2016) or sulfate ions (Li *et al*. 2016).

In the aforementioned studies, the raw materials used to produce MOC were acquired from industrial suppliers, whereas other researchers have used magnesite ($MgCO_3$) ore to produce one of the raw materials (MgO) used to prepare MOC (El-Mahllawy *et al*. 2012; Tan *et al*. 2015). The suitability of dolomite ore for producing MOC was evaluated by Kacker *et al*. (1970).

[1]Researcher, Department of Mining Engineering, Çukurova University, Balcali/Adana, Turkey.
*Corresponding author, *E-mail:* maltiner@cu.edu.tr
[2]Professor, Department of Mining Engineering, Çukurova University, Balcali/Adana, Turkey.

Table 1. Mix proportion of MOC with various molar ratios.

$MgO/MgCl_2$ (M)*	$H_2O/MgCl_2$ (H)*					
	13	14	15	16	17	18
4.74	X	X	X	X		
5.52	X	X	X	X	X	
6.06	X	X	X	X	X	
7.97		X	X	X	X	X

They partially calcined dolomite at 750°C for 2 h and then added it to an $MgCl_2$ solution to prepare MOC. $CaCO_3$ acted a filler in the mix proportion of their MOC.

The methodology adopted in the present work differs from those of the aforementioned studies in which dolomite was used to produce MOC. In the present work, the raw materials necessary for producing MOC were obtained from dolomite by leaching–precipitation–evaporation–pyrohydrolysis processes. The influences of the $MgO/MgCl_2$ and $H_2O/MgCl_2$ molar ratios and the amount of phosphoric acid (H_3PO_4) on the properties of MOC were investigated in detail. The compressive strength, bulk density, and water immersion test were measured for each prepared MOC. In addition, SEM examination was performed to determine the change of selected MOC microstructures. The thermal conductivity, fire strength, flexural strength, and dimensional stability properties of the final MOC product was determined.

2. Experimental procedure

2.1. Raw materials and mix proportion

The starting materials (MgO and $MgCl_2{\cdot}6H_2O$) for producing MOC were obtained from dolomite. The chemical composition of the dolomite used for producing raw materials to prepare the MOC was 19.84% MgO, 31.37% CaO, and 48.2% CO_2. The purity of each raw material was quite high (99.9%) because the impurities had been removed after the leaching process (Altiner *et al*. 2016). During the leaching process, CO_2 gas was stored in a lab-scale gasometer for use in the subsequent carbonation process that was conducted to remove Ca^{2+} ions as synthetic aragonite crystals from the leachate solution (Altiner and Yildirim 2016) and obtain an Mg-rich solution. Afterwards, the solution was crystallized at 130°C using an evaporator (Altiner and Yildirim 2016) to obtain $MgCl_2$ crystals. Finally, MgO particles were prepared through pyrohydrolysis and calcination processes (temperature: 650°C, reaction time: 270 min). The production of MgO from dolomite will be explained in a future study. The obtained materials were subsequently used to produce MOC.

P5 is known to be the most stable MOC phase at ambient temperature; the $MgO/MgCl_2$ and $H_2O/MgCl_2$ molar ratios were determined for this purpose (**Table 1**). Given the molar ratios in **Table 1**, $MgCl_2{\cdot}6H_2O$ was first dissolved in tap water to obtain a magnesium chloride solution. Thereafter, MgO particles were added to the solution, which was stirred gently (80 rpm) by a mechanical stirrer for 15 min to obtain homogeneous MOC pastes. The prepared pastes were poured into Plexiglas molds using a vibration table and cured for 24 h at ambient temperature. The initial and final setting times of the MOC samples were determined via a Vicat apparatus according to standard ISO 9597:2008. After hardening for 24 h, each MOC sample was removed from its mold and cured in air (20°C and 50% relative humidity) for 7 days.

In this paper, the mix proportions of MOC samples given in **Table 1** are denoted as M_xH_y (where M = nMgO/$n$$MgCl_2$, H = $n$$H_2O$/$n$$MgCl_2$) (Li and Chau 2007). For example, the notation $M_{4.74}H_{14}$ indicates the MOC with $MgO/MgCl_2$ and $H_2O/MgCl_2$ molar ratios of 4.74 and 14, respectively.

2.2. Effects of H_3PO_4 addition on water resistance of MOC

The 7-day MOC (20 × 20 × 20 mm^3) samples were immersed in tap water for 10 days to determine their water resistance. By the end of the tenth day, the compressive strength value of the MOC samples was determined. The water resistance coefficient (W_R) was calculated using Eq. 1 (Liu *et al*. 2015).

$$W_R = \frac{CSI_{im}}{CSI_{7d}} \quad (1)$$

where W_R is the water resistance coefficient, CSI_{im} is the compressive strength value of the MOC immersed in tap water for 10 days (MPa), and CSI_{7d} is the compressive strength value of the MOC sample on day 7 (MPa).

The amounts of Cl^- ions before and after the immersion tests were measured via the silver nitrate ($AgNO_3$) titration method (Association 1992). Given all of the experimental results, a small amount of H_3PO_4 (1–4% of H_3PO_4/MgO ratio) was added to the magnesium chloride solution before the addition of MgO to produce the selected mix proportion of MOC. The influences of the H_3PO_4 addition on the water resistance of the selected MOC were then investigated using all of the aforementioned procedures described in this paper.

2.4. Testing and characterization methods

2.4.1. Physico-mechanical properties of MOC

The compressive strength value (CSV) of each 7-day MOC sample (20 × 20 × 20 mm^3) was determined according to TS EN 12390-10 (2010). The loading speed was 50 N/s. Each test was repeated two times to reduce the experimental error of the CSVs of the MOC samples.

In addition, the bulk density of 7-day MOC prepared with various M_xH_y molar ratios was determined according to standard TS EN-1097-6 (2015).

2.4.2. Evaluation of microstructures of selected MOC

After the CSV test, four selected samples with molar ratios of $M_{4.74}H_{13}$, $M_{5.52}H_{13}$, $M_{6.06}H_{14}$, and $M_{7.92}H_{15}$ selected from all of the samples were ground using an agate mortar for XRD and SEM examination. The microstructures on the fractured surface of each 7-day MOC were evaluated using a scanning electron microscope (Zeiss 55 and Philips XL 30S FEG) after the samples were coated with gold particles. The crystallographic properties of selected MOC were determined using a Rigaku X-ray diffractometer equipped with Cu Ka radiation in the 2θ range of 15 – 60° with a 0.02 step size.

2.4.3. Determination of final MOC product properties

The thermal conductivity (TC) of the final MOC product was measured through the hot wire method (ASTM 2013). The TC is the property of material to conduct heat, whereas the fire strength test is used to evaluate concrete behavior in terms of heat conduction in the event of a fire outbreak. The rate at which heat is transferred from a hot surface to the cold surface of a concrete component was determined through this method.

In addition, concrete can be classified on the basis of the experimental results of the fire strength tests. **Fig. 1** shows the apparatus designed for the fire strength test. The average surface temperature of each MOC product was measured using a laser infrared thermometer with K-type thermocouple functionality (CEM, DT8835). The temperature of the bottom, middle, and upper points of the final MOC product were measured before the test. Afterwards, the fire source (900°C) was exposed to the bottom surface of the final product (70 × 70 × 10 mm^3) at a distance of 10 mm for 10 min. To represent the surface temperature of the unexposed side of the product, the temperature of each product was measured at the same points at 30-s time intervals during the fire test. The average temperature of the unexposed side of each MOC product was calculated. The heat transfer rate of the MOC was determined using the following equation (Anonymous 2016). The loss of MOC after each test was further weighted.

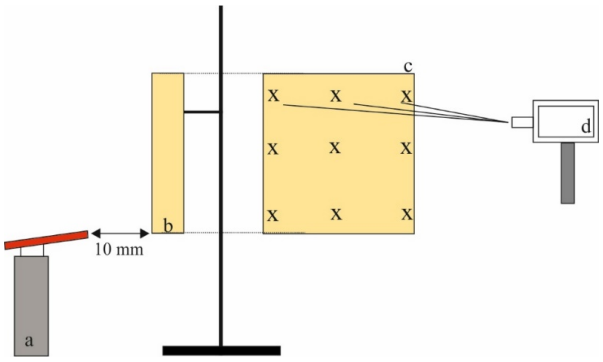


Fig 1. Experimental apparatus for fire strength tests: a) fire source, b) MOC sample, c) unexposed surface of the MOC sample, d) thermometer (points where the temperature of the MOC surface measured are marked with an x).

$$R_{\text{Rate}} = \lambda \cdot A \cdot (\frac{P_{T2} - P_{T1}}{P_K}) / 1000 \quad (2)$$

where, R_{Rate} is the heat transfer rate of MOC (J/s), λ is the thermal conductivity value of MOC (W/m·K), A is the surface area of MOC (m^2), P_{T2} is the measured temperature of exposed surface by fire source (K), P_{T1} is the measured temperature of unexposed surface of MOC (K), P_K is the thickness of MOC (m).

The flexural strength value (FSV) of the final MOC product were determined according to TS EN 12390-5 (2010). Furthermore, the dimensional changes in the final MOC product at 70°C after 48 h were determined (TSE EN 1604, 2013). The length, width and thickness of MOC was measured before and after the dimensional change test. The volumetric change shows the dimensional stability of MOC cement. If the volumetric change was small, no structural problems related to cement would be observed.

3. Results and discussion

3.1. Effects of molar ratio of M_xH_y on production of MOC

The possible chemical reactions in the ternary system of MgO – $MgCl_2$ – H_2O for producing MOC were explained in detail in previous studies (Dehua and Chuanmei 1999; Karimi and Monshi 2011). We therefore do not discuss the chemical reactions that occur during the hardening of MOC here. We determined that the initial setting of each MOC paste began after 30 min, whereas the final setting time of the paste varied between 170 and 195 min depending on its mix proportion.

The presence of Cl^- ions was an important parameter in the MOC manufacturing process; changing the $MgCl_2$ concentration in the MOC paste led to the undesired MOC phase, as shown in the ternary phase diagram of the MgO–$MgCl_2$–H_2O system (**Fig. 2**). Each mix proportion of MOC was prepared to obtain P5. However, P3 can sometimes be obtained in the case of MOC samples with an $M_{4.74}$ ratio, as evident in the phase diagram. Depending on the M_x ratio, more MgO than needed can be added to the mix proportion of MOC. However, excess MgO is not harmful and may act as a filler (Karimi and Monshi 2011). These findings were confirmed by the XRD analyses given in **Fig. 3.** Excess MgO and $Mg(OH)_2$ crystals were determined. Similarly, higher H_2O levels were required for workability of the MOC paste. The concentration of Cl^- ions, which can lead to corrosion problems, was kept to a minimum in

Table 2. Bulk density of MOC with various molar ratios.

$MgO/MgCl_2$ (M)*	$H_2O/MgCl_2$ (H)*					
	13	14	15	16	17	18
4.74	1.86	1.83	1.71	1.69		
5.52	1.84	1.84	1.78	1.72	1.70	
6.06	1.89	1.85	1.86	1.86	1.80	
7.97		1.98	1.94	1.89	1.88	1.88

the MOC pastes (Sglavo *et al*. 2011). These ratios strongly affected the microstructure of the resulting MOC when MgO and H_2O were added in greater-than-necessary amounts to the MOC paste, as shown in **Fig. 4**.

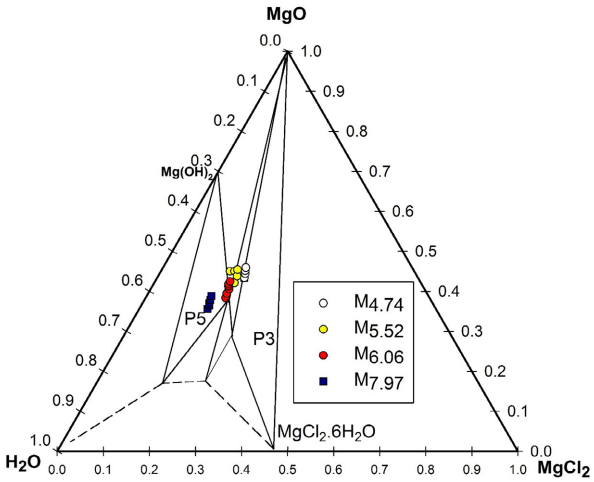


Fig 2. Phase diagram of the ternary system of MgO–$MgCl_2$–H_2O for producing MOC.

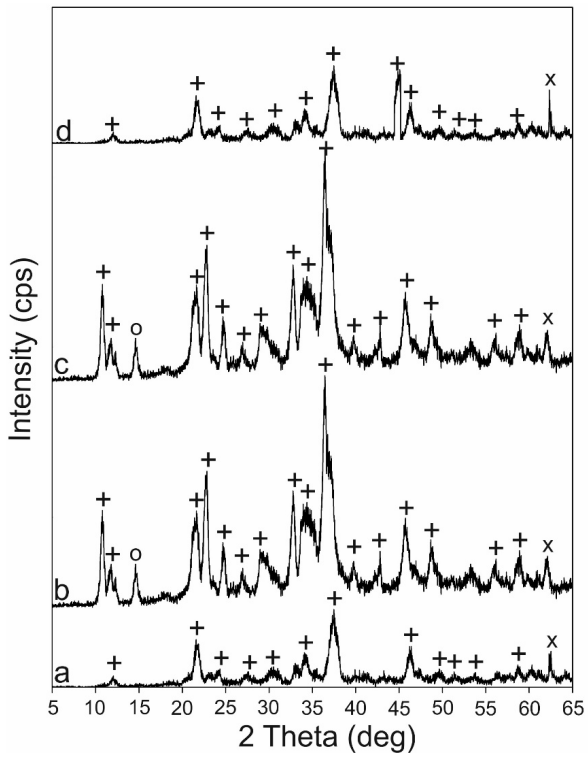


Fig 3. XRD curves of MOC: a) $M_{4.74}H_{13}$, b) $M_{5.52}H_{13}$, c) $M_{6.06}H_{14}$, d) $M_{7.92}H_{15}$ (+ : P5, o: $Mg(OH)_2$, x: MgO).

To obtain needle-shaped MOC crystals, the MOC molar ratio should be $M_{6.06}H_{14}$ (**Fig. 4(c)**). With the addition of more MgO to the MOC, the needle-like crystals of MOC disappeared at the molar ratio of $M_{7.92}H_{15}$ because the pores in the MOC were filled by excess MgO particles (**Fig. 4(d)**). The intergrowth of needle-shaped crystals of the MOC led to an increase of its strength value (Karimi and Monshi 2011). The obtained results given in **Fig. 5** are consistent with those of previous studies. The highest CSV of the 7-day MOC samples was 87.7 MPa in the case of $M_{6.06}H_{14}$, which contains needle-shaped crystals (**Fig. 4(c)**). The CSVs of the 7-day MOC samples started to decrease with disappearing needle crystals of the MOC when excess MgO was added. For instance, the CSV of MOC $M_{7.92}H_{15}$ was found to be 80 MPa. Even though needle-shaped crystals appeared in MOC samples $M_{4.74}H_{13}$ and $M_{5.52}H_{13}$, their CSVs were 42 and 77 MPa, respectively. These lower CSVs are related to the amount of MgO in the MOC samples. The bulk density of MOC prepared in various molar ratios was in the range of 1.71 and 1.98 g/cm^3 as shown in **Table 2**.

3.2. Effects of H_3PO_4/MgO ratio on water resistance of MOC

MOC is not durable in water, although an increase of the $MgO/MgCl_2$ molar ratio (M_x) leads to an increase of its water resistance (Dehua and Chuanmei 1999). A possible decomposition reaction of MOC in water is represented as the following equation:

$$Mg_3(OH)_5Cl\cdot 4H_2O \rightarrow 2.5Mg(OH)_{2(s)} + 0.5Mg^{2+}_{(aq)} + Cl^-_{(aq)} + 4H_2O \quad (3)$$

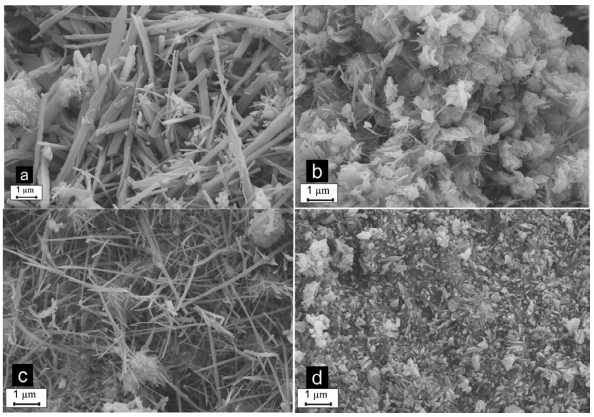


Fig 4. SEM images of MOC samples prepared at various molar ratios: a) $M_{4.74}H_{13}$, b) $M_{5.52}H_{13}$, c) $M_{6.06}H_{14}$, and d) $M_{7.92}H_{15}$.

Table 3. Water resistance coefficients of MOC samples prepared at various molar M_xH_y molar ratios.

MgO/$MgCl_2$ (M)*	$H_2O/MgCl_2$ (H)*					
	13	14	15	16	17	18
4.74	0.48	0.35	0.12	0.10		
5.52	0.32	0.21	0.18	0.18	0.13	
6.06	0.24	0.21	0.21	0.18	0.17	
7.97		0.00	0.44	0.40	0.30	0.26

XRD analyses shown in **Fig. 6** reveal that the phase of selected MOC decomposed after immersion in water for 10 days. The MOC crystals converted to $Mg(OH)_2$ thereafter. This is in line with the SEM examination. It is clear that the needle-shaped crystals of MOC disappeared after immersion in water for 10 days because the MOC decomposed (**Fig. 7**). A comparison of SEM images of the MOC before and after immersion in water (for instance, **Fig. 4(a)** and **Fig. 7(a)**) clarified the disappearance of the needle-shaped crystals in the MOC. Furthermore, the presence of Cl^- ions in the water after the immersion test indicates the decomposition of the MOC. The amounts (by mass) of Cl^- ions dissolved from the MOC were 50.7% for $M_{4.74}H_{13}$, 56.1% for $M_{5.52}H_{13}$, 51.2% for $M_{6.06}H_{14}$, and 37.2% for $M_{7.97}H_{15}$ after the immersion test.

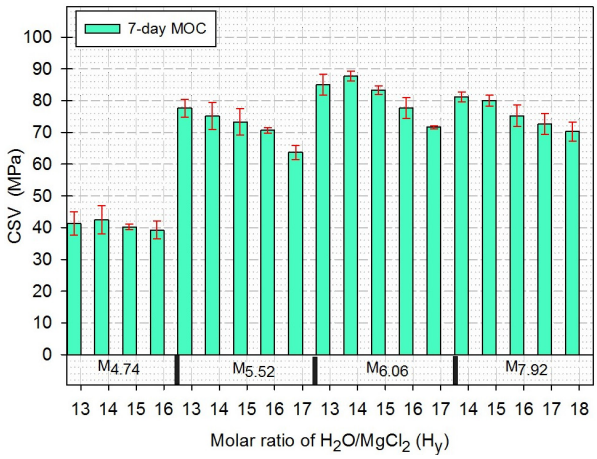


Fig 5. Compressive strength values of MOC samples prepared at various M_xH_y ratios.

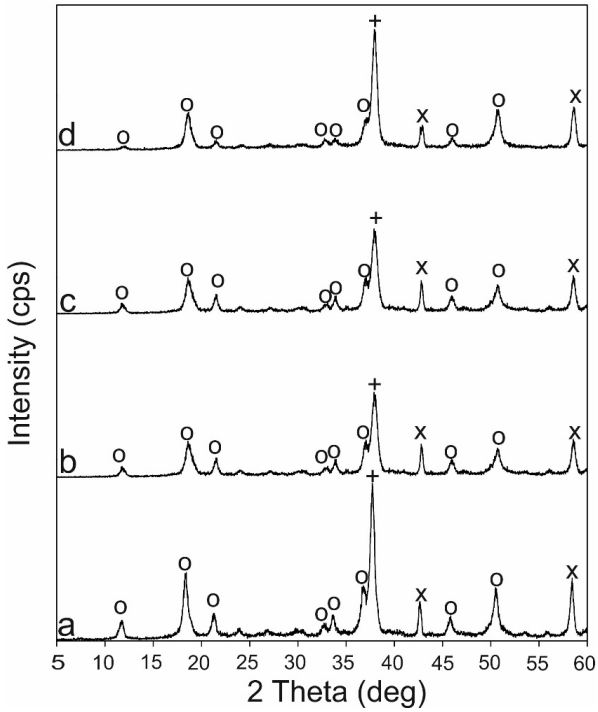


Fig 6. XRD curves of MOC samples after immersion tests: a) $M_{4.74}H_{13}$, b) $M_{5.52}H_{13}$, c) $M_{6.06}H_{14}$, d) $M_{7.92}H_{15}$ (+: P5, o: $Mg(OH)_2$, x: MgO).

Unfortunately, the decomposition of the MOC samples led to a decrease of their CSVs. A comparison of the CSV value of an MOC before and after an immersion test is shown in **Fig. 8**. The CSV of the MOC ($M_{6.06}H_{14}$) decreased from 87.7 MPa to 18.05 MPa, which corresponds to a 79% reduction in the CSV. The CSV of the MOC was found to be higher depending on its M_x molar ratio after the immersion test. However, the MOC prepared in the molar ratio of $M_{7.97}H_{14}$ was scattered as the cracks were formed on the surface of MOC during the immersion test. The water resistance coefficient (W_R) of each MOC is listed in **Table 3.**

Therefore, H_3PO_4 additives were added at concentrations ranging from 1 to 4% (by weight of MgO) to the mix proportion of the MOC composition ($M_{6.06}H_{14}$) with the highest CSV to increase its W_R (Deng 2003; Tan *et al*. 2014; Gapparova *et al*. 2015). Thereafter, the CSVs of the MOC samples with various H_3PO_4/MgO ratios were determined; the results are shown in **Fig. 9.** An increase of the H_3PO_4/MgO ratio in the MOC led to an increase of the W_R of the MOC. After the immersion tests, the CSV of the MOC with 4% H_3PO_4/MgO was found to be 61 MPa. The W_R of this MOC was calcu-

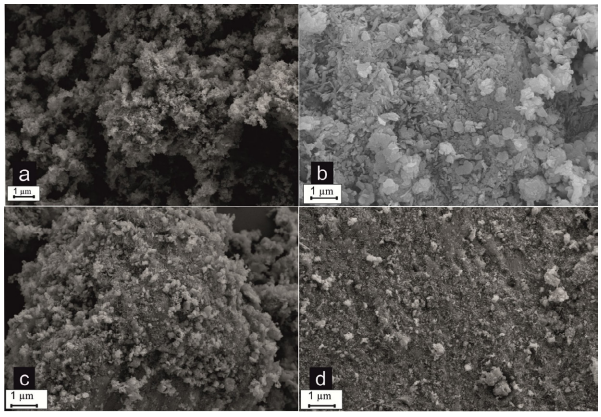


Fig 7. SEM images after immersion tests of MOC samples prepared at various molar ratios: a) $M_{4.74}H_{13}$, b) $M_{5.52}H_{13}$, c) $M_{6.06}H_{14}$, and d) $M_{7.92}H_{15}$.

lated to be 0.69 (= 61/87.7).

Lu *et al*. (1994) have reported that a gelatinous structure formed on the surface of an MOC because of the presence of PO_4^{3-} anions in its composition; they also reported that the pores of the MOC were already coated by the gelatinous layer before the immersion test. Consequently, water could not diffuse inside the MOC, preventing the decomposition of its structure (Tan *et al*. 2014). These findings were confirmed by the XRD examination shown in **Fig. 10**. The characteristic peaks belonging to P5 of MOC were determined. MgO and $Mg(OH)_2$ peaks were further observed. No crystal peaks related to phosphor were observed due to an adding small amounts of H_3PO_4 to the mix proportion of MOC.

In the present work, the structure of the MOC did not decompose after immersion in water, as shown in the SEM images (**Fig. 11**). Needle-shaped crystals were observed in each SEM image. However, Cl^- ions were detected after the immersion test. The amounts of Cl^- ions dissolved from the MOC varied between 12.2 and 22.65% (by mass) depending on its H_3PO_4/MgO ratio. With respect to the SEM images in **Fig. 11**, more pronounced crystals in the MOC were observed when the

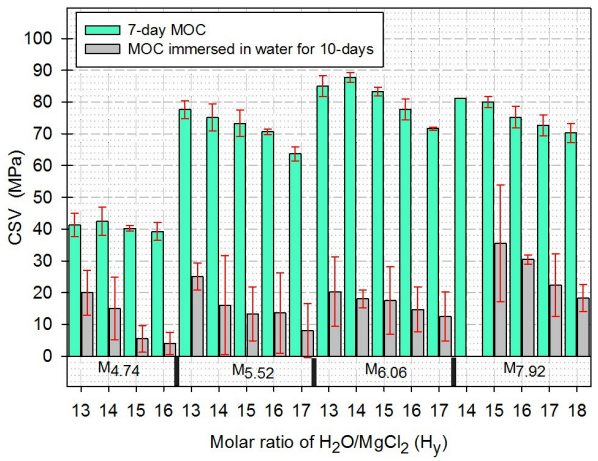


Fig 8. Comparison of the CSVs of MOC before and after an immersion test.

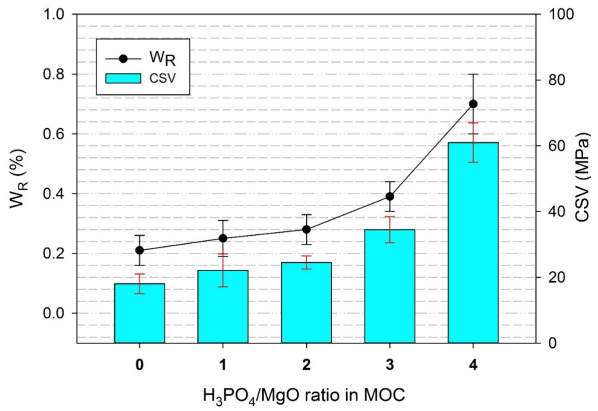


Fig 9. Influences of the H_3PO_4/MgO ratio in MOC ($M_{6.06}H_{14}$) on its water resistance coefficient (W_R) and compressive strength value (CSV).

Table 4. Dimensional stability of final MOC product (thickness of 10 mm).

Parameter	Before	After	Difference (%)
Length (mm)	71.74	71.45	0.40
Width (mm)	71.12	71.04	0.12
Thickness (mm)	9.68	9.40	2.89

H_3PO_4/MgO ratio in the MOC was 4%. The 7-day MOC ($M_{6.06}H_{14}$, H_3PO_4/MgO ratio: 4%) is hereafter referred to as the final product.

3.3. Determination of final MOC product properties

The flexural strength value (FSV) of MOC cement varied between 2 – 14 MPa depending on its production condition (Misra and Mathur 2007; Zhou and Li 2012; Wen *et al*. 2014). In this paper, the FSV of the final MOC product was found to be 4.22 MPa that was in good agreement with those studies. The increase of curing days leads to increase the FSV of the final product as indicated in the previous study (Wen *et al*. 2014). Then, the FSV of the final MOC product (thickness of 10 mm) in this paper will increase in an extended curing times. The final MOC product was stable at 70°C. There was no considerable difference determined on the product after 48 h as shown in **Table 4.**

The TCV of the final MOC product was found to be 1.202 W/(m·K), which is consistent with the results of a previous study (Xu *et al*. 2016). This value is one of the most important properties of an MOC. The heat source was exposed for 10 min to the surface of the final MOC

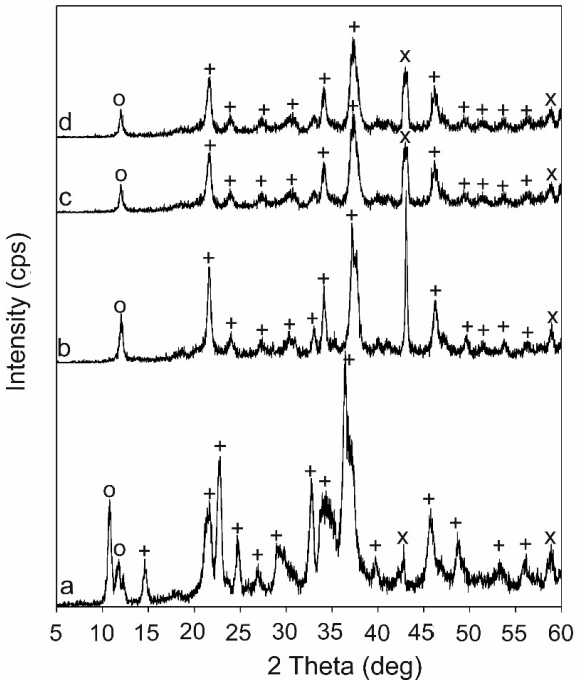


Fig 10. XRD curves of MOC samples containing various ratios of H_3PO_4/MgO by weight after the immersing test: a) 1% b) 2%, c) 3%, and d) 4% (+: P5, o: $Mg(OH)_2$, x: MgO).

Table 5. Changes in surface temperature of final MOC product after the fire resistance test.

Thickness (mm)	Temperature (°C)			Weight loss (%)
	Initial	Final	Differences	
10	15	382	367	12.28
25		45	30	11.15
40		42	27	8.65
70		20	5	2.03

product ($M_{6.06}H_{14}$, H_3PO_4/MgO: 4%) prepared with a thickness of 10, 25, 50 and 70 mm. The temperature of the unexposed surface of the MOC with a thickness of 10 mm increased from 15°C to 382°C after the test. However, this value tends to decrease with increasing thickness value of MOC. The differences in the temperature of the exposed surface of the MOC were determined before and after the test. **Table 5** gives the experimental results of the fire resistance tests. No ignition was observed and that the flame did not advance on the surface of the final MOC product.

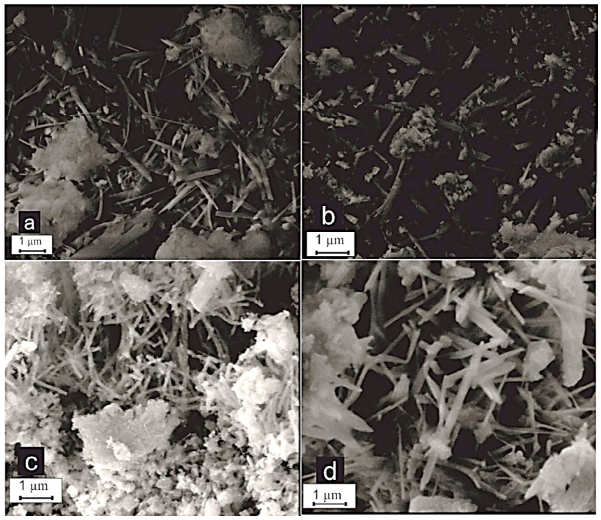


Fig 11. SEM images of MOC ($M_{6.06}H_{14}$) containing various ratios of H_3PO_4/MgO by weight after the immersing test: a) 1%, b) 2%, c) 3%, and d) 4%.

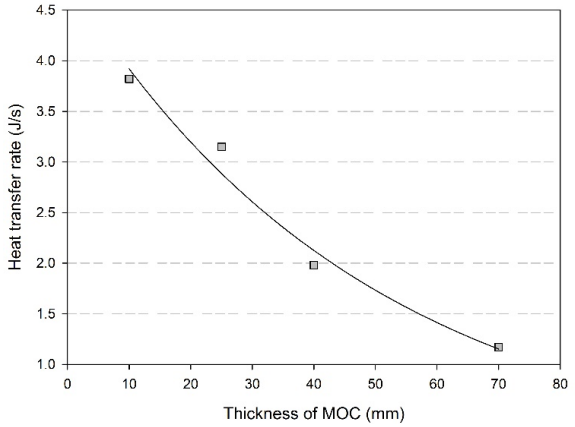


Fig 12. Heat transfer rate of MOC depending on its thickness.

When the thickness of that product was ≥25 mm, the differences between exposed and unexposed surfaces of the final MOC product were found to be lower 30°C and the weight loss was below 11%. The heat transfer rate of the final MOC product was greatly influenced by its thickness (**Fig. 12**). When the thickness of MOC increased to 70 mm from 10 mm, the R_{rate} decreased to 1.17 J/s from 3.82 J/s. Considering these experimental results, the final MOC product was classified as A1 construction product according to the TSE 13501-1+A1 2013 (TSE 2013).

4. Conclusions

This paper shows that dolomite ore can be evaluated as starting materials for producing magnesium oxychloride cement (MOC). Leaching–carbonation–evaporation–pyrohydrolysis processes were carried out to prepare the starting materials (MgO and $MgCl_2$). The best experimental results in terms of physico-mechanical properties, XRD and SEM examination were obtained when the mix proportion of MOC was $M_{6.06}H_{14}$. To increase the W_R of the MOC, a small amount of H_3PO_4 (4% of MgO by weight) was added. The W_R of the MOC was found to be 0.69, which is an acceptable value for the composite concrete.

Consequently, approximately 2.49 t of dolomite is required to produce 1 t of MOC based on the experimental results obtained in this work. This value would be decreased with adding of filler to produce lightweight MOC product. In a next study, the influences of using expanded perlite and exfoliated vermiculite as fillers on the property of MOC product will be investigated. During the production per 1 t of MOC, 1.38 t of synthetic aragonite ($CaCO_3$) and 0.58 t of CO_2 with a high purity would be obtained as byproducts, which are highly demanded in many industrial areas.

Acknowledgement

This work was supported by the Research Fund Project [grant number MMF2013D18, ID:606] of Çukurova University.

References

Altiner, M. and Yildirim, M., (2017). "Production and characterization of synthetic aragonite prepared from dolomite by eco-friendly leaching–carbonation process." *Advanced Powder Technology*, 28(2), 553-564.

Altiner, M. and Yildirim, M., (2016). "Production of magnesium chloride ($MgCl_2$) from Aydıncık/İçel dolomites" *Ç.Ü. Fen ve Mühendislik Bilimleri Dergisi*, 34(3). (in Turkish)

Altiner, M., Yildirim, M. and Yilmaz, T., (2016). "Leaching of Mersin/Aydincik dolomite ore in hydrochloric acid. dissolution rates" *Physicochem. Probl. Miner. Process*, 52(2), 536-550.

Anonymous. (2016). "Rates of heat transfer." from

http//www.physicsclassroom.com/class/thermalP/Lesson-1/Rates-of-Heat-Transfer.

Association, A. P. H., (1992). "*APHA method 4500-Cl, standards methods for the examination water and wastewater*."

ASTM, (2013). "*ASTM C1113 / C1113M - 09, Standard test method for thermal conductivity of refractories by hot wire* (Platinum Resistance Thermometer Technique)."

Chau, C. K. and Li, Z., (2007). "Microstructures of magnesium oxychloride." *Materials and Structures,* 41(5), 853-862.

Chau, C. K. and Li, Z., (2008). "Accelerated reactivity assessment of light burnt magnesium oxide." *Journal of the American Ceramic Society*, 91(5), 1640-1645.

Dehua, D. and Chuanmei, Z., (1999). "The formation mechanism of the hydrate phases in magnesium oxychloride cement." *Cement and Concrete Research*, 29, 1365-1371.

Deng, D., (2003)., "The mechanism for soluble phosphates to improve the water resistance of magnesium oxychloride cement." *Cement and Concrete Research*, 33(9), 1311-1317.

El-Mahllawy, M. S., Hassan, H. A., and Kandeel, A. M., (2012). "The influence of aggregate type on the physcio-mechnical properties of magnesia cement pastes." *Chemical engineering journal*, 1(1), 4-10.

Gapparova, K. M., Khudyakova, T. M., Verner, V. F. and Atanbayeva, L. S., (2015). "Production of waterproof composite magnesia cement on the basis of local mineral resources." *Modern Applied Science*, 9(3), 309-315.

Harper, F. C., (1967). "Effect of calcination temperature on the properties of magnesium oxides for use in magnesium oxychloride cements." *J. App. Chem*., 17, 5-10.

Hendriks, C. A., Worrell, E. Jager, D. de, Blok, K. and Riemer, P., (2004). "Emission reduction of greenhouse gases from the cement industry." In: *IEA greenhouse gas control technologies conference*, 1-11.

Imbabi, M. S., Carrigan, C. and McKenna, S., (2012). "Trends and developments in green cement and concrete technology." *International Journal of Sustainable Built Environment*, 1(2), 194-216.

ISO, (2008). "*ISO 9597, Cement -- Test methods -- Determination of setting time and soundness*."

Kacker, K. P., Mehrotra, G. S., and Rai, M., (1970). "Petrographic and thermal evaluation of dolomite for the manufacture of magnesium oxychloride cement." *J. App. Chem*., 20, 189-193.

Karimi, Y. and Monshi, A., (2011). "Effect of magnesium chloride concentrations on the properties of magnesium oxychloride cement for nano SiC composite purposes." *Ceramics International*, 37(7), 2405-2410.

Li, Y., Li, Z., Pei, H. and Yu, H., (2016). "The influence of $FeSO_4$ and KH_2PO_4 on the performance of magnesium oxychloride cement" *Construction and Building Materials*, 102, 233-238.

Li, Z. and Chau, C. K., (2007). "Influence of molar ratios on properties of magnesium oxychloride cement." *Cement and Concrete Research*, 37(6), 866-870.

Liu, Z., Wang, S., Huang, J., Wei, Z., Guan, B. and Fang, J., (2015). "Experimental investigation on the properties and microstructure of magnesium oxychloride cement prepared with caustic magnesite and dolomite." *Construction and Building Materials*, 85, 247-255.

Lu, H. P., Wang, P. L., and Jiang, N. X., (1994). "Design of additives for water-resistant magnesium oxychloride cement using pattern recognition." *Materials Letters*, 20(3-4), 217-223.

Misra, A. K. and Mathur, R., (2007). "Magnesium oxychloride cement concrete." *Bull. Mater. Sci.*, 30(3), 239-246.

Qiao, H.-x., Gong, W., Shi, Y.-y., Wanjiru, M. E. and Dong, J.-m., (2016). "Experimental study on magnesium oxychloride cement concrete." *Emerging Materials Research*, 5(2), 248-255

Qiao, H., Cheng, Q. Jinlei, W. and Yingying, S., (2014). "The application review of magnesium oxychloride cement." *Journal of Chemical and Pharmaceutical Research*, 6(5), 180-185.

Sorel, S., (1867). "On a new magnesium cement". *CR Acad Sci*, 65, 102-104.

Sglavo, V. M., Genua, F. De, Conci, A., Ceccato, R. and Cavallini, R., (2011). "Influence of curing temperature on the evolution of magnesium oxychloride cement." *Journal of Materials Science*, 46(20), 6726-6733.

Tan, Y., Liu, Y. and Grover, L. M., (2014). "Effect of phosphoric acid on the properties of magnesium oxychloride cement as a biomaterial." *Cement and Concrete Research*, 56, 69-74.

Tan, Y., Liu, Y., Zhao, Z., Paxton, J. Z. and Grover, L. M., (2015). "Synthesis and in vitro degradation of a novel magnesium oxychloride cement." *J Biomed Mater Res A*, 103(1), 194-202.

TSE, (2010a). "*TS EN 12390-2, Testing hardened concrete - Part 2, Making and curing specimens for strength tests*."

TSE, (2010b). "*TS EN 12390-5, Testing hardened concrete - Part 5, Flexural strength of test specimens*."

TSE, (2013a). "*TS EN 1604, Thermal insulating products for building application determination of dimensional stability under specified temperature and humidity conditions*."

TSE, (2013b). "*TS EN 13501-1+A1, Fire classification of construction products and building elements - Part 1, Classification using data from reaction to fire tests*."

TSE, (2015). "*TS EN 1097-6, Tests for mechanical and physical properties of aggregates - Part 6, Determination of particle density and water*

absorption."

Wen, J., Yu, H., Li, Y., Wu, C. and Dong, J., (2014). "Effects of citric acid on hydration process and mechanical properties of thermal decomposed magnesium oxychloride cement." *Journal of Wuhan University of Technology-Mater. Sci. Ed.,* 29(1), 114-118.

Wu, C., Yu, H., Zhang, H., Dong, J., Wen, J. and Tan, Y., (2015). "Effects of phosphoric acid and phosphates on magnesium oxysulfate cement." *Materials and Structures*, 48(4), 907-917.

Xu, B., Ma, H., Hu, C. and Li, Z., (2016). "Influence of cenospheres on properties of magnesium oxychloride cement-based composites." *Materials and Structures,* 49(4), 1319-1326.

Xu, B., Ma, H., Hu, C., Yang, S. and Li, Z., (2016). "Influence of curing regimes on mechanical properties of magnesium oxychloride cement-based composites." *Construction and Building Materials*, 102, 613-619.

Zhang, C. and Deng, D., (1994). "Research on the water-resistance of magnesium oxychloride cement I, the stability of the reaction products of magnesium oxychloride cement in water." *J. Wuhan Univ. Technol. Mater. Sci. Ed.*, 9, 51-59.

Zhou, X. and Li, Z,. (2012). "Light-weight wood–magnesium oxychloride cement composite building products made by extrusion." *Construction and Building Materials*, 27(1), 382-389.

Zhu, J., Ye, N., Liu, J. and Yang, J., (2013). "Evaluation on hydration reactivity of reactive magnesium oxide prepared by calcining magnesite at lower Temperatures." *Industrial & Engineering Chemistry Research*, 52(19), 6430-6437.